Layered optical tomography of multiple scattering media with combined constraint optimization

Bingzhi Yuan, Toru Tamaki, Takahiro Kushida, Bisser Raytchev, Kazufumi Kaneda[1],
Yasuhiro Mukaigawa, Hiroyuki Kubo[2]

Abstract

In this paper, we proposed an improved optical scattering tomography for optically dense media. We model a material by many layers with voxels, and light scattering by a distribution from a voxel in one layer to other voxels in the next layer. Then we write attenuation of light along a light path by an inner product of vectors, and formulate the scattering tomography as an inequality constraint optimization problem solved by an interior point method. To improve the accuracy, we solve simultaneously four configurations of a multiple-scattering tomography, however, this would increase the computational cost by a factor of four if we simply solved the problem four times. To reduce the computation cost, we introduce a quasi-Newton method to update the inverse of a Hessian matrix used in the iteration of the interior point method. We show experimental results with numerical simulation for evaluating the proposed method and comparisons with our previous work.

1. Introduction

In this paper we describe a method for scattering optical tomography of highly scattering media. Unlike X-ray computed tomography (CT) which uses X-ray penetrating human body, optical tomography uses visible or infrared light sources and has been developed over the last decades [1, 2]. Diffuse optical tomography (DOT) [3] is a kind of optical tomography widely used today. Our current paper aims to develop an optical tomography method that uses infrared light input and observed outgoing light at the opposite side of the body, shown as in Figure 1(a), like as a source-detector configuration that X-ray CT uses. The incident light is however heavily scattered inside a medium when the medium is optically thick; this usually happens in the case of human body. This problem is called *scattering tomography* and recently studied in optics [4, 5], physics [6, 7], computer vision [8, 9], and even computer graphics [10, 11].

Light scattering is modeled usually by the radiative transfer equation (RTE) [12, 13] in physics and optics, and by the volume rendering equation [10, 14] for a time-independent case, which has been developed in in computer graphics. A forward problem of light scattering uses those equations and is therefore studied both in physics for simulation [12, 13] and in graphics for rendering [15, 16, 17, 18]. An inverse problem of light scattering — this is often called inverse scattering or scattering tomography — has been studied in many different approaches, for example, approximations of RTE [4], single scattering assumption [6, 7], and uniform media approximation [10]. Often scattering is assumed to be weak [4] or single [6, 7] because highly scattering media and multiple scattering is difficult to analyze.

We present a method of *multiple* scattering tomography whose approach is based on an approximation of the volume rendering equation in order to deal with highly scattering media and multiple scattering. In this paper, we extend our previous work [9] for improving accuracy and efficiency. The model of light scattering of our method is based on the path integral [17, 19, 20] developed in graphics community. Since the scattering model with path integral is so general, we take the following assumptions (see Fig. 1(b)) : (1) multiple (not single) scattering is dominant, (2) forward scattering is also dominant relative to backward scattering, (3) a material consists of many parallel layers made of voxels, and (4) light is scattered from one layer to another because forward scattering is assumed be dominant. Combining these assumptions together, we develop a constraint optimization problem to solve the scattering tomography.

Contributions of this paper are summarized as follows:

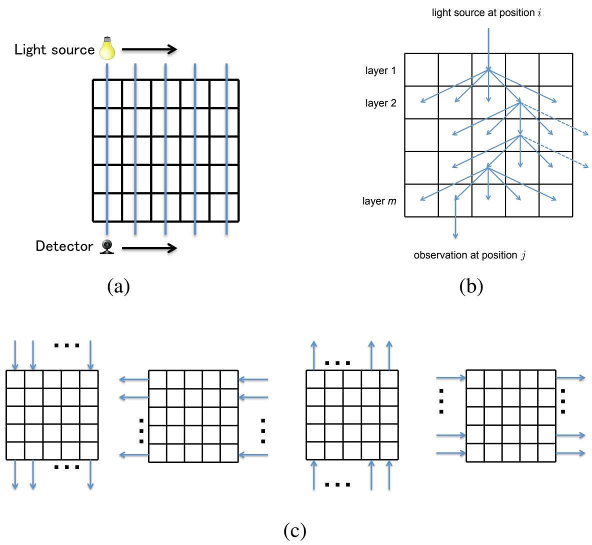

Figure 1. Configurations of light sources and observations. (a) Source-detector configuration of CT. (b) A single configuration with the layers model. A light source at position i emits light to the first layer, then the light is scattered to the next layer. At the last layer, output is observed at each position j. (c) Four configurations. The object is fixed while the light source and detector are rotated by 90 degrees.

- We develop an optimization method to solve simultaneously four configurations a multiple-scattering tomography (shown in Figure 1(c)), while the previous work [9] is limited to a single configuration. This significantly improves the quality of results.
- We introduce a quasi-Newton method to efficiently solve the optimization problem.

We will describe the scattering model in section 2 as a forward and inverse models. The developed constraint optimization problem and algorithm to solve it with an interior point method with quasi-Newton is shown also in section 2. Experimental results of numerical simulation are shown in section 3. In the simulation, we demonstrate that accuracy of the results increases, and computation time decreases to about 30% compared to the previous work. This improvement seems promising, while the material used in the simulation is of the size 10 by 10 in 2D and also the number of configurations are four instead of 360 as in CT because of the inherent difficulty of multiple scattering.

2. Method

In this section, we first describe the forward problem; how light goes through a medium in terms of path integral. Then we describe the developed algorithm to solve the the inverse problem of scattering tomography.

2.1.Forward model

Our layered model is shown in Figure 1(b). A scattering material is a 2D grid consisting of N layers, each of which has M voxels; $\boldsymbol{x}_{n,m}$. Our aim is to estimate each voxel's *extinction coefficients*, $\sigma_t(\boldsymbol{x}_{n,m})$, which describe how much light is attenuated at that voxel. To this end, we emit light from a light source to the first layer at position i from the top side of the material. The light is attenuated and scattered to the next layer, while some portion of light goes outside. What we observe is the light I_{ij} going outside from the bottom layer at position j. By changing incident and outgoing positions (i, j), we have a set of observations I_{ij}. We describe the scattering and attenuation models below.

We use a simple scattering model [9] from voxel i at layer n to voxel j at layer $n+1$:

$$p_s(\boldsymbol{x}_{n,i}, \boldsymbol{x}_{n+1,j}) = Ce^{\frac{\|\boldsymbol{x}_{n,i}-\boldsymbol{x}_{n+1,j}\|^2}{\sigma^2}}, \qquad (1)$$

where $\boldsymbol{x}_{n,i}$ is the coordinate of the center of voxel i at layer n, and $C = \frac{1}{\sqrt{2\pi\sigma^2}}$. The Gaussian model of scattering [21] encodes the scattering coefficient (or scattering cross section) and the phase function. It has parameter σ^2 describing how broad the light is scattered. This model results in a scattering factor c_{ijk} of a particular path;

$$c_{ijk} = \prod_{n=1}^{N-1} p_s, \qquad (2)$$

where (i, j, k) is index of kth path $(k = 1, \ldots, M^{N-2})$ that starts at i and ends at j.

Attenuation of light is modeled by the integral of extinction coefficients along a path. For a segment of a path (Fig. 2(a)) from voxel i at layer n to voxel j at layer $n+1$, the attenuation factor can be exactly written as the following form of exponential decay;

$$p_t(\boldsymbol{x}_{n,i}, \boldsymbol{x}_{n+1,j}) = e^{-\int_0^1 \sigma_t((1-s)\boldsymbol{x}_{n,i}+s\boldsymbol{x}_{n+1,j})ds}, \qquad (3)$$

where $\sigma_t(\boldsymbol{x})$ is extinction coefficient at $\boldsymbol{x}$.

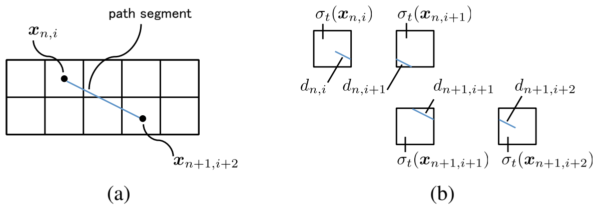

Figure 2. A path segment (a) from $\boldsymbol{x}_{n,i}$ to $\boldsymbol{x}_{n+1,i+2}$ and corresponding four subsegments (b) only in contributing voxels.

In our 2D layered model, extinction coefficients are assumed to be constant in each voxel. Hence this integral over the path segment can be transformed into the sum of the length, $d_{n,i}$, over a voxel i in layer n multiplied by the extinction coefficient, $\sigma_t(\boldsymbol{x}_{n,i})$, of that voxel, as follows [9]:

$$p_t(\boldsymbol{x}_{n,i}, \boldsymbol{x}_{n+1,j}) = e^{-\sum_{\hat{n}=n}^{n+1} \sum_{\hat{i}} d_{\hat{n},\hat{i}} \sigma_t(\boldsymbol{x}_{\hat{n},\hat{i}})}. \tag{4}$$

Here we somehow abuse the notation: $d_{\hat{n},\hat{i}}$ is the length of the part where the path segment (from voxel i at layer n to voxel j at layer $n+1$) passes across voxel $\hat{i}$ at layer $\hat{n}$. An example is shown in Fig. 2(b). Here, a path segment from $\boldsymbol{x}_{n,i}$ to $\boldsymbol{x}_{n+1,i+2}$ is decomposed into four subsegments, hence four voxels only contribute to compute the attenuation (3). Other voxels are ignored and corresponding $d_{\hat{n},\hat{i}}$ in (4) are zero. Therefore we can write the exponential decay along a path as a sum of extinction coefficients.

The attenuation at each layer is accumulated as the light goes along a path from layer to layer. To simplify the notation, we introduce a vector notation; Let $\boldsymbol{d}_{ijk}$ be a path represented as a *length* vector that consists of $d_{n,i}$ of all voxels and $\boldsymbol{\sigma}_t$ be a vector of extinction coefficients of $\sigma_t(\boldsymbol{x}_{n,i})$. Now the attenuation factor a_{ijk} of a particular path (i,j,k) can be written as

$$a_{ijk} = \prod_n p_t = e^{-\boldsymbol{d}_{ijk}^T \boldsymbol{\sigma}_t}. \tag{5}$$

Observations I_{ij} are the sum of contributions of all paths;

$$I_{ij} = \sum_{k=1}^{M^{N-2}} I_0 \; c_{ijk} \; a_{ijk}, \tag{6}$$

where I_0 is the intensity of incident light. Because the observation is the sum of all path contributions, this model is called a path integral [17, 19, 20] while in our case integral is replaced wit summation.

2.2.Inverse model

Next we describe our inverse problem.

By changing a pair of (i,j), the positions of incident and outgoing points of light, we have M^2 observations I_{ij} and equations to solve the following least squares problem:

$$\min_{\boldsymbol{\sigma}_t} f_0, \quad f_0 = \sum_{i=1}^{m} \sum_{j=1}^{m} |I_{ij} - \sum_{k=1}^{m^{m-2}} I_0 c_{ijk} \; e^{-\boldsymbol{d}_{ijk}^T \boldsymbol{\sigma}_t}|^2, \tag{7}$$

under $2MN$ constraints

$$0 \preceq \boldsymbol{\sigma}_t \preceq u, \tag{8}$$

where the symbol $\preceq$ denotes generalized inequality that every elements in a vector must satisfy the inequality. The lower bound comes from the fact that the extinction coefficient must be positive, and the upper bound is for numerical stability to exclude unrealistic values to be estimated.

As shown in Figure 1(c), we have four configurations of light sources and detectors. To use all of them at the same time, we add corresponding four cost functions to form a single function f_0; there are four different sets of observations I_{ij} and paths ijk while they all share the same variables $\boldsymbol{\sigma}_t$ to be estimated. This makes us to use the same problem (7) in a single formulation at the expense of additional (factor of four) computation cost.

We solve the above optimization problem with inequality constraints by using an interior point method with barrier functions [22]. The developed algorithm is shown in Algorithm 1. It iteratively solves unconstrained optimization problems with modified cost function (9) with barrier functions to keep solutions feasible. The unconstrained optimization problems are also solved iteratively, we call them iteration *inner loops*, and iterations of them *outer loops*.

We introduce a quasi-Newton method to reduce the computation cost of the inner loop. Newton method is known to be computationally expensive, which was used in our previous work [9], because it keeps Hessian and computes its inverse for computing a direction at each step. Instead, we use a quasi-Newton method, more specifically, Broyden–Fletcher–Goldfarb–Shanno (BFGS) algorithm to update the inverse of Hessian. We will show in the experiments that computation time decreases compared to the previous work whereas results are much improved.

Algorithm 1: Proposed algorithm for the inverse problem.

Input: Parameters $\mu > 1$, $\epsilon > 0$, and $t = t_{\text{init}} > 0$.
Data: A feasible initial solution $\boldsymbol{\sigma}_t = \mathbf{0}$, Hessian inverse $H^{-1} = I$.
Result: $\boldsymbol{\sigma}_t$.

repeat`// outer loop: interior point`
  $t \leftarrow \mu t$
  Set a barriered cost function;

$$f_1(t) = \; t f_0 - \sum_l (\log(\sigma_{tl}) + \log(u - \sigma_{tl})), \tag{9}$$

  where σ_{tl} is l-th element of $\boldsymbol{\sigma}_t$.
  $k \leftarrow 0$, $H_k^{-1} \leftarrow H^{-1}$, ${\boldsymbol{\sigma}_t}^k \leftarrow \boldsymbol{\sigma}_t$.
  repeat`// inner loop: quasi-Newton`
    Update H_k^{-1} with BFGS.
    Compute direction: $-H_k^{-1} \nabla f_1({\boldsymbol{\sigma}_t}^k)$.
    Perform line search to find step size α.
    Update estimate ${\boldsymbol{\sigma}_t}^{k+1} \leftarrow {\boldsymbol{\sigma}_t}^k - \alpha H_k^{-1} \nabla f_1({\boldsymbol{\sigma}_t}^k)$.
    $k \leftarrow k + 1$.
  until *converge*;
  $H^{-1} \leftarrow H_k^{-1}$, $\boldsymbol{\sigma}_t \leftarrow {\boldsymbol{\sigma}_t}^k$.
until $\frac{2MN}{t} \geq \epsilon$;

3. Experimental results

We evaluate the proposed method by numerical simulation. Four kinds of materials of the size 10×10 shown in Figure 3(a) are used. Each material has almost homogeneous extinction coefficients (in light gray) except few voxels with much higher coefficients (in darker gray), which means those voxels absorb light much more than others. Parameters are set as follows: $\sigma^2 = 1.0$ for scattering; $u = 1.0$ for the upper bound; $t_{\text{init}} = 1.0$, $\mu = 1.5$, and $\epsilon = 10^{-2}$ for interior point.

Estimated results are shown in Figure 3(b) and (c): results in the second row (b) are obtained by previous work [9], while results in the third row (c) are by our proposed method. Our results (c) are much closer to the ground truth (a) and better than the previous work (b). This is also confirmed by qualitative results in terms of root mean squares error (RMSE) shown in Table 1. Table 2 shows computation time spent by the previous work and proposed method; it is roughly reduced to 30% (by our unoptimized code in MATLAB on a PC with Intel Xeon E5 2GHz).

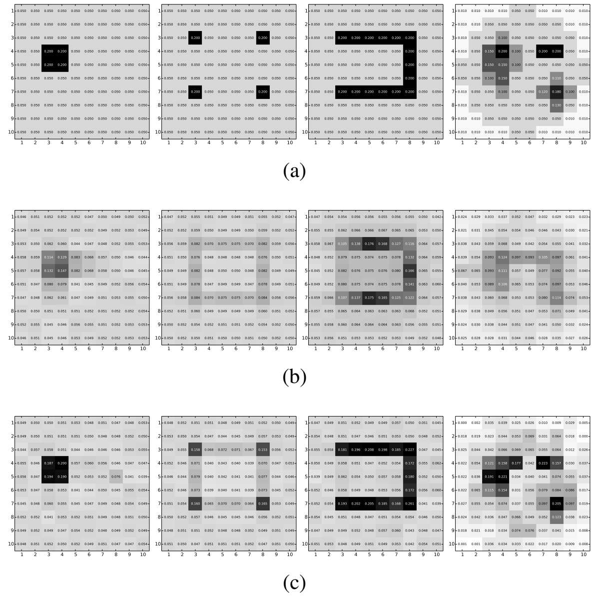

Figure 3. Simulation results for $\sigma^2 = 1.0$. (a) Ground truth of four materials 1, 2, 3, and 4. (b) Results of [9]. (c) Results of our method. Values in each voxel are estimated value of $\boldsymbol{\sigma}_t$, and darker gray represents larger value.

Table 1. RMSEs of results for four materials. The order is the same with Figure 3(b) and (c).

method	1	2	3	4
Fig. 3(b) [9]	0.016978	0.02731	0.043248	0.030447
Fig. 3(c) ours	0.004987	0.01213	0.010154	0.022141

Values of the cost function f_0 in Eq. (7) are shown in Figure 4. At each iteration of the outer loop of Algorithm 1, the difference between observation and the model, Eq. (7), decreases and becomes smaller than 10^{-5} at the convergence.

4. Conclusions

In this paper, we have proposed an improved scattering tomography with a layered model. Based on the assumptions we made for simplifying a scattering material, we have formulated the inverse model as a constraint nonlinear least squares problem. Then we solved it by interior point method with a quasi-Newton

Table 2. Computation time (in seconds) of results for four materials in Figure 3(b) and (c).

method	1	2	3	4
Fig. 3(b) [9]	191.334	162.035	197.519	195.628
Fig. 3(c) ours	55.602	55.602	70.531	76.773

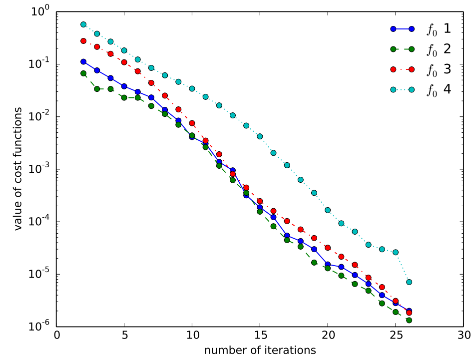

Figure 4. Cost function values f_0 over iterations of outer loop. Numbers of f_0 are the order in Figure 3(c): 1 is the left most, and 4 is the right most.

method. In the experiments, results were much more improved than the previous work as well as computational cost is decreased. Currently our simulation is limited to discretized 2-dimensional media, however the method can be applied to 3-dimensional media. Also more larger size of grids will be used in future work.

References

[1] Pedro González-Rodríguez and Arnold D. Kim. Comparison of light scattering models for diffuse optical tomography. *Optics Express*, 17(1):8756–8774, 2009.

[2] S. R. Arridge. Optical tomography in medical imaging. *Inverse Problems*, 15(R41–93), 1999.

[3] A. P. Gibson, J. C. Hebden, and S. R. Arridge. Recent advances in diffuse optical imaging. *PHYSICS IN MEDICINE AND BIOLOGY*, 50:R1–R43, 2005.

[4] Vadim Y. Soloviev and Simon R. Arridge. Optical tomography in weakly scattering media in the presence of highly scattering inclusions. *Biomed. Opt. Express*, 2(3):440–451, Mar 2011.

[5] W. Cong and G. Wang. X-ray scattering tomography for biological applications. *Journal of X-Ray Science and Technology*, 19:219–227, 2011.

[6] Lucia Florescu, John C. Schotland, and Vadim A. Markel. Single-scattering optical tomography. *PHYSICAL REVIEW E*, 79:036607–1–10, 2009.

[7] Lucia Florescu, Vadim A. Markel, and John C. Schotland. Single-scattering optical tomography: Simultaneous reconstruction of scattering and absorption. *Phys. Rev. E*, 81:016602, Jan 2010.

[8] Yasunori Ishii, Toshiya Arai, Yasuhiro Mukaigawa, Jun'ichi Tagawa, and Yasushi Yagi. Scattering tomography by monte carlo voting. In *IAPR International Conference on Machine Vision Applications*, 2013.

[9] T. Tamaki, B. Yuan, B. Raytchev, K. Kaneda, and Y. Mukaigawa. Multiple-scattering optical tomography with layered material. In *Signal-Image Technology Internet-Based Systems (SITIS), 2013 International Conference on*, pages 93–99, Dec 2013.

[10] Ioannis Gkioulekas, Shuang Zhao, Kavita Bala, Todd Zickler, and Anat Levin. Inverse volume rendering with material dictionaries. *ACM Trans. Graph.*, 32(6):162:1–162:13, November 2013.

[11] Yoshinori Dobashi, Wataru Iwasaki, Ayumi Ono, Tsuyoshi Yamamoto, Yonghao Yue, and Tomoyuki Nishita. An inverse problem approach for automatically adjusting the parameters for rendering clouds using photographs. *ACM Transactions on Graphics*, 31(6), 2012.

[12] S. Chandrasekhar. *Radiative transfer*. Dover, 1960.

[13] Akira Ishimaru. *Wave Propagation and Scattering in Random Media*. Academic Press, 1978.

[14] Eva Cerezo, Frederic Pérez, Xavier Pueyo, Francisco J. Seron, and François X. Sillion. A survey on participating media rendering techniques. *The Visual Computer*, 21(5):303–328, 2005.

[15] Eric P. Lafortune and Yves D. Willems. Rendering participating media with bidirectional path tracing. In *Proceedings of the Eurographics Workshop on Rendering Techniques '96*, pages 91–100, London, UK, UK, 1996. Springer-Verlag.

[16] Henrik Wann Jensen and Per H. Christensen. Efficient simulation of light transport in scences with participating media using photon maps. In *SIGGRAPH '98*, pages 311–320. ACM, 1998.

[17] Mark Pauly, Thomas Kollig, and Alexander Keller. Metropolis light transport for participating media. In *Eurographics Workshop on Rendering Techniques*, pages 11–22, 2000.

[18] Yonghao Yue, Kei Iwasaki, Bing-Yu Chen, Yoshinori Dobashi, and Tomoyuki Nishita. Unbiased, adaptive stochastic sampling for rendering inhomogeneous participating media. *ACM Transactions on Graphics*, 29(6), December 2010.

[19] Eric Veach and Leonidas J. Guibas. Metropolis light transport. In *Proceedings of the 24th Annual Conference on Computer Graphics and Interactive Techniques*, SIGGRAPH '97, pages 65–76, New York, NY, USA, 1997. ACM Press/Addison-Wesley Publishing Co.

[20] Simon Premože, Michael Ashikhmin, and Peter Shirley. Path integration for light transport in volumes. In *Proceedings of the 14th Eurographics Workshop on Rendering*, EGRW '03, pages 52–63, Aire-la-Ville, Switzerland, Switzerland, 2003. Eurographics Associa-

tion.
[21] Simon Premože, Michael Ashikhmin, Ravi Ramamoorthi, and Shree Nayar. Practical rendering of multiple scattering effects in participating media. In *Eurographics Symposium on Rendering*, 2004.
[22] Stephen Boyd and Lieven Vandenberghe. *Convex Optimization*. Cambrige Univesity Press, 2004.